ECOGRAPHY

Research

Landscape scale variation in the hydrologic niche of California coast redwood

Emily J. Francis, Gregory P. Asner, Katharine J. Mach and Christopher B. Field

E. J. Francis (https://orcid.org/0000-0002-7123-781X) ✉ (emily.francis@austin.utexas.edu), Dept of Integrative Biology, Univ. of Texas at Austin, Austin, TX, USA. – G. P. Asner (https://orcid.org/0000-0001-7893-6421), Center for Global Discovery and Conservation Science, Arizona State Univ., Tempe, AZ, USA. – K. J. Mach (https://orcid.org/0000-0002-5591-8148), Rosenstiel School of Marine and Atmospheric Science, Univ. of Miami, Miami, FL, USA, and Leonard and Jayne Abess Center for Ecosystem Science and Policy, Univ. of Miami, Coral Gables, FL, USA. – C. B. Field (https://orcid.org/0000-0002-1684-8247), Stanford Woods Inst. for the Environment, Stanford Univ., Stanford, CA, USA.

Ecography
43: 1305–1315, 2020
doi: 10.1111/ecog.05080

Subject Editor: Nathalie Pettorelli
Editor-in-Chief: Miguel Araújo
Accepted 26 May 2020

Topoclimatic diversity within forest landscapes can underlie variation in water availability, which may correspond to patterns in habitat suitability of tree species with differing hydrologic niches. However, the trade-off between the collection of data at a fine grain size over large spatial extents has limited comprehensive analyses of landscape scale variation in habitat suitability. We present a fine scale analysis of the roles of topographic gradients in moisture availability, soil water storage and fog frequency in the spatial pattern of habitat suitability for coast redwood *Sequoia sempervirens*, at 10 m resolution across 34 800 ha and three landscapes spanning approximately one-third of redwood's latitudinal range. A new 10 m resolution presence-absence map derived from airborne imaging spectroscopy was used to characterize current redwood distributions in three landscapes. Access to belowground moisture was assessed through four measures calculated from a high-resolution LiDAR digital elevation model, soil water storage was mapped from the USDA Soil Survey Geographic Database, and fog frequency was calculated from MODIS cloud cover data. Access to belowground moisture and fog predicted variation in suitability as redwood habitat from 22–75% and predicted redwood presence and absence at 10 m resolution with 63–74% accuracy. Across all three landscapes, redwood density consistently decreased with increasing interpolated height above a stream (IHAS), but the role of other predictors varied among the sites. Our results challenge previous assumptions that redwood habitat suitability within much coarser resolutions (800 m × 800 m) can be described by a single value. The elevated habitat suitability of sites close to streams suggests that these sites should be evaluated for their potential to become microrefugia within landscapes that may become climatically-unsuitable for redwoods at a regional scale.

Keywords: DEM, Global Airborne Observatory, hydrologic niche, microclimate, redwood, species distribution model

NORDIC SOCIETY OIKOS

www.ecography.org

© 2020 The Authors. Ecography published by John Wiley & Sons Ltd on behalf of Nordic Society Oikos
This is an open access article under the terms of the Creative Commons Attribution License, which permits use, distribution and reproduction in any medium, provided the original work is properly cited.

Introduction

Understanding the factors that determine species' range boundaries has been a longstanding goal of biology (Grinnell 1917, Guisan and Thuiller 2005, Soberon 2007). Species distribution models (SDMs) seek to explain species' ranges through correlations of observed range limits with measurements of environmental variation (Elith and Leathwick 2009). The rapid rate of climate change (Loarie et al. 2009) has hastened the need for SDMs with the capacity to forecast shifts in species' habitats (Araújo et al. 2019). Tree species may be particularly vulnerable to climate change because they are long-lived organisms that are limited to migration through reproduction. Trees have been predicted to undergo significant and widespread range shifts and range contractions in response to climate change over the next century (McKenney et al. 2007, Meier et al. 2011, Iverson et al. 2013), but evidence that their populations are migrating to track shifts in climate is lacking (Zhu et al. 2012).

Widespread, drought-induced forest mortality events (Allen et al. 2010), concentrated at species' dry range edges (Anderegg et al. 2019), suggest that declining water availability may be a key mechanism in tree species' range contraction events in the future. Trees vary in their tolerance for drought and are adapted to particular hydrologic niches, defined by a tolerance for anoxia at their wetter range edge and a tolerance for low water potentials at their drier range edge (Silvertown et al. 1999, 2015). Warming temperatures as a result of climate change have increased the rate of evaporation from soil and leaf surfaces, thereby reducing water availability and shifting species' hydrologic niches in space (Breshears et al. 2013). Climate models consistently indicate that increasing temperatures will continue to intensify droughts for many regions across the globe (IPCC 2013), posing an impending threat to standing trees and the ecosystem services they provide (Anderegg et al. 2013).

Water availability is affected by processes that occur at multiple ecological scales, from that of an individual leaf, to landscape, regional and global levels. The amount of precipitation affects inputs of water, temperature controls the loss of water to the atmosphere through evapotranspiration, and variation in topography and soil affect the movement and residence time of water across landscapes (McLaughlin et al. 2017). To accommodate this variation, SDMs for plants have been developed at continental (Thuiller et al. 2005), regional (McKenney et al. 2007) and landscape scales (Dawson 1990, Douda et al. 2012, Pradervand et al. 2014, Letten et al. 2015, García-Baquero et al. 2016). However, the physical and computational challenge of collecting and analyzing large volumes of data results in a trade-off between resolution and spatial extent in SDMs. Thus, species distribution models operated at a regional scale may fail to identify potential microrefugia, microsites that may continue to support species when the surrounding landscape has been predicted to become climatically unsuitable (Dobrowski 2011, Franklin et al. 2013, Lenoir et al. 2017). On the other hand, species distribution models operated at a sufficiently high resolution to identify microrefugia are necessarily limited in spatial extent, and therefore may not cover a representative portion of the species' habitats.

Recent advances in airborne remote sensing have the potential to overcome some of the limitations of the extent/grain size trade off in SDMs, by providing high-resolution data over a larger extent than is practical with data collected from field surveys. Estimating topographic variation from airborne LiDAR (Light Detection and Ranging) digital elevation models (DEMs) that corresponds to variation in water availability at fine spatial scales is a common practice (Beven and Kirkby 1979, Moore et al. 1991, McCune and Dylan 2002, Nobre et al. 2011). However, while the use of environmental predictors from DEMs has become commonplace, the use of species distribution data at a comparable resolution and extent has lagged (He et al. 2015). Species distribution data collected from field survey plots or compiled from field observations have dominated in SDM studies, even in those that use remotely-sensed environmental predictor data (Jetz et al. 2012). However, it was recently demonstrated that combining airborne imaging spectroscopy data with a small subset of field data in a classification model is an effective method for mapping the presence and absence of tree species at the resolution of individual trees over thousands of hectares of forest (Baldeck et al. 2015). SDM approaches using tree species distribution maps produced from airborne imaging spectroscopy have not yet been widely implemented (but see Andrew and Ustin 2009 for an example with an invasive weed).

Coast redwoods *Sequoia sempervirens* are an important case study for understanding the role of water availability in habitat suitability. The tallest tree on earth is a redwood standing at 112.7 m (Koch et al. 2004), and some redwood trees are thousands of years old (Carroll et al. 2014). Redwoods have high demands for water, reported to be more than 600 l d^{-1} for a 45 m individual (Dawson 1998). A prior species distribution model for coast redwoods using presence-only occurrence data and climate data at 800-m resolution predicted that climatically-suitable habitat for redwoods may significantly contract at the southern end of the redwood distribution by 2030 under a middle-of-the-road climate change scenario (RCP 4.5, Fernandez et al. 2015). However, redwood forests are situated in topo-climatically complex landscapes, which are likely to contain significant and unquantified variation in redwood habitat suitability at spatial scales finer than 800 m. In addition to variation in access to water due to topographic position, spatial patterns of fog introduce additional variation in the hydrologic conditions in redwood forests. Fog is a thick layer of low clouds that forms over the Pacific and is advected onto land during the summer months (Johnstone and Dawson 2010). The presence of fog increases atmospheric humidity and reduces evapotranspiration, and in some locations, fog can provide precipitation through fog drip (Sawaske and Freyberg 2015). However, in sites that are above the height of the fog bank

or on east-facing slopes where fog is blocked by a mountain, both of these types of fog moisture are absent and redwoods must rely on water stored in the water table, in unsaturated soil, or in weathered bedrock, particularly during summers and drought years.

Here, we investigated the roles of topoedaphically-mediated variability in belowground moisture and fog on redwood habitat suitability at the landscape scale. We tested the generality of site-level results by comparing across three sites that covered approximately one-third of the latitudinal distribution of the species. Specifically, we asked: 1) does landscape scale variation in access to moisture influence the distribution of redwoods? 2) How do different sources of moisture, specifically fog moisture and topoedaphically-mediated belowground moisture, influence redwood habitat suitability? 3) What can the current hydrological niche of coast redwood tell us about landscape scale variation in redwood habitat suitability under climate change, in comparison with a previous study of redwood habitat suitability at a regional scale?

Material and methods

Study species and sites

This study was conducted at three different redwood forest landscapes. Big Basin is the southernmost landscape, has the lowest mean annual precipitation at 1093 mm and highest mean annual temperature at 14.72°C. Mt Tamalpais (hereafter Mt Tam) is a mid-latitude site north of San Francisco, with 1160 mm mean annual precipitation and mean annual temperature of 13.96°C. It includes Muir Woods National Monument, an old-growth redwood forest. Jackson Forest is the northernmost landscape, has the highest mean annual precipitation at 1214 mm and lowest mean annual temperature at 13.14°C. All three sites have a history of logging and forest stands of various ages (Supplementary material Appendix 1 Supplementary text).

This study used data collected from the Global Airborne Observatory (GAO; formerly Carnegie Airborne Observatory). The GAO is an airborne laboratory carrying four mapping sensors that include a visible-to-shortwave infrared imaging spectrometer (VSWIR), a visible-to-near infrared spectrometer (VNIR) and a light detection and ranging scanner (LiDAR) (Asner et al. 2012). The GAO collected imaging spectroscopy and LiDAR data from all three forests in late July 2016. LiDAR data was collected at 0.5–2 m resolution and the imaging spectrometer data was collected at 1–2 m resolution, depending on the site (Francis and Asner 2019). The total area covered by all three landscapes exceeded 34 800 ha, and spanned approximately one-third of the latitudinal distribution of redwood (Fig. 1a). Mean annual temperature and mean annual precipitation of each site were calculated from PRISM 30-yr normals from 1981–2010 at 4-km resolution as the average value at each site (Daly et al. 2008).

Redwood presence and absence map

We used a redwood presence and absence dataset at 10-m resolution derived from the GAO airborne imaging spectroscopy data and field collected training data. Full details on the map have been described previously (Francis and Asner 2019), but we note relevant details here. Field training data were collected from 362 redwood crowns and 268 non-redwood crowns, and were used to train a model to classify pixels as 'redwoods' or 'other' across a hyperspectral image. The classification model, when tested on a dataset that was not included in model development, mapped redwood pixels with a 98% true positive rate (TPR) and 2% false positive rate (FPR) at Big Basin, 90% TPR and 1% FPR at Muir Woods, and 81% TPR and 3% FPR at Jackson Forest (Francis and Asner 2019). The model was then applied to the hyperspectral image for each site. The final map provides data on the presence or absence of a redwood canopy at 10 m resolution over 34 800 ha. Pixels located on water bodies and in urban areas were removed prior to further analysis.

Access to belowground moisture

We calculated four topographic measures of access to belowground moisture, specifically topographic wetness index, curvature, heat load index (HLI) and interpolated height above the stream (IHAS), from each site's LiDAR-derived digital elevation model (DEM). Topographic wetness index is the ratio of the area upslope of a cell and the local slope, and it is a proxy for the amount of water input to a cell and infiltration rate (Beven and Kirkby 1979). Curvature is a measure of concavity versus convexity and indicates whether water is more likely to infiltrate into the soil or flow over a cell (Moore et al. 1991, Porres de la Haza and Pardo Pascual 2002). HLI approximates the amount of radiation received by a slope, based on slope aspect and steepness. Higher HLI indicates a lower heat load (McCune and Dylan 2002). The topographic wetness index, curvature and HLI were all calculated using the Geomorphometry and Gradients metrics toolbox in ArcMap 10.1 (Cushman et al. 2010).

IHAS is similar to the height above the nearest drainage (HAND, Nobre et al. 2011) and relative slope position (Vaughn et al. 2015). To calculate it, we delineated a drainage network for each site from the digital elevation model based on the method of O'Callaghan and Mark (1984), using the ArcGIS Hydrology Toolset. The stream elevation at each point was calculated from a linear interpolation of stream elevation at the stream points (Nobre et al. 2011). At edges, nearest neighbor rather than linear interpolation was used. IHAS was calculated as the difference between the actual elevation and the interpolated stream elevation for each cell.

We included a fifth index, soil available water storage, from the US Dept of Agriculture Natural Resource Conservation Survey (NRCS) Soil Survey Geographic Database (SSURGO). Its units are centimeters of potential water storage in the top 150 cm of soil (Soil Survey Staff 2004). SSURGO data are gathered from field surveys as well

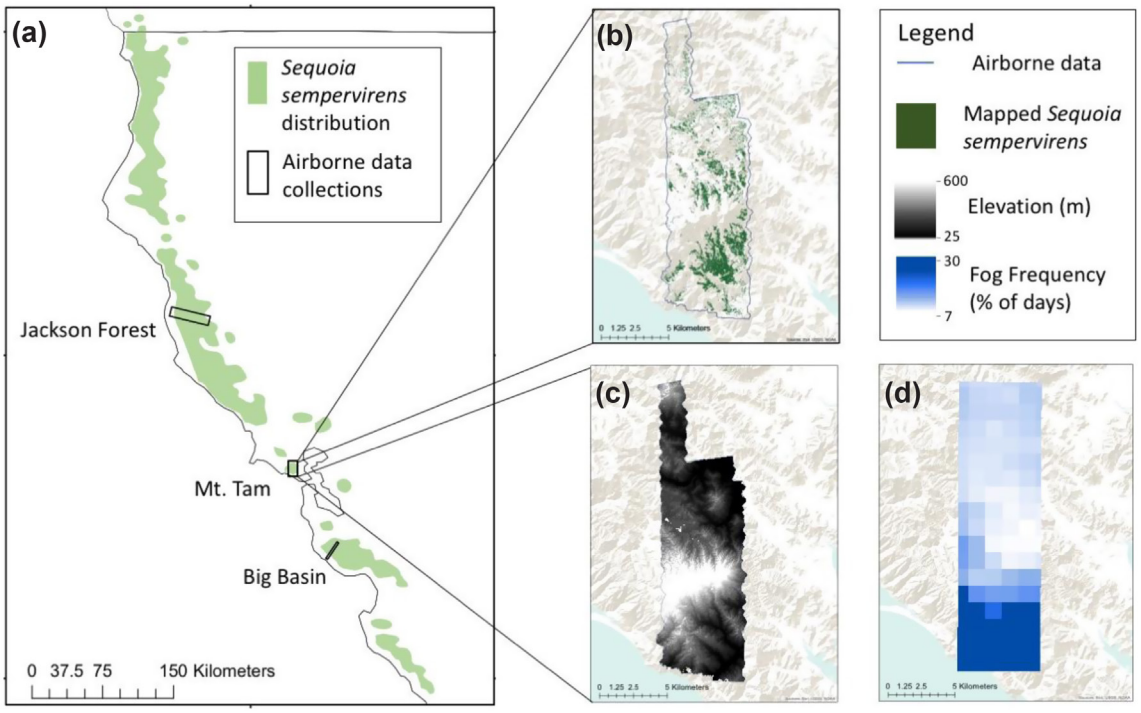


Figure 1. The Global Airborne Observatory (formerly Carnegie Airborne Observatory) collected imaging spectroscopy and LiDAR data from three redwood landscapes in California on a latitudinal gradient (a). Close-ups of one of the landscapes (Mt Tam; insets (b), (c) and (d)) show the data used for each site. Inset (b): presence and absence of redwood *Sequoia sempervirens* trees at 10 m resolution, as mapped with a machine learning image classification on the airborne imaging spectroscopy data. Inset (c): LiDAR-derived digital elevation model from which four metrics of belowground moisture variation were calculated at 10 m resolution. Inset d: MODIS-derived map of fog frequency at 1 km resolution, calculated as the percentage of days in July and August with cloud cover at 10:30 am. The redwood distribution data at 1 km resolution in (a) is from Little (1971).

as comparison with geologic, topographic and vegetation maps. We included it in order to incorporate variation in soil type which could not be captured by topography alone, however, we note that in some cases, vegetation type may have helped to guide soil-type mapping. We therefore include this potential circularity as a source of uncertainty in our interpretation (Davis et al. 2010).

Access to fog moisture

Fog frequency was estimated from MODIS cloud cover data at 1-km resolution (Fischer et al. 2009, Baguskas et al. 2014). During the months of July and August, low-level marine stratus clouds comprise more than 75% of clouds on the coast of California (Iacobellis and Cayan 2013). For simplicity, we assumed that all clouds at our study sites during July and August were fog. The MODIS cloud flag collects data at 10:30 AM (Fischer et al. 2009). We calculated fog probability for each pixel as the proportion of days that were marked as 'cloudy' or 'mixed' during July and August from 2000–2016. This fog map differentiates among sites that have access to any type of fog moisture from those that do not, and does not differentiate among sites that have access to water from fog drip from those that are exposed to increased relative humidity and shading. All predictor variables were re-sampled to match the 10 m resolution of the redwood presence-absence data prior to analysis.

Modeling

A classification and regression tree (CART) approach was used to model the effects of fog, topography and soils (Table 1) on redwood distributions (Elith and Graham 2009, Morin and Thuiller 2009, Evans et al. 2010, Heikkinen et al. 2012). Specifically, we used a boosted regression tree (BRT). BRTs are advantageous because they are non-parametric, can efficiently model non-linear relationships with large datasets, and are robust to redundant predictor variables (Elith et al. 2008). All analyses were done with the Scikit-learn package in Python ver. 2.7.13 (Pedregosa et al. 2011), with settings of 100 trees, a maximum depth of 4, a learning rate of 0.01 and a least square loss function.

Model assessment

All model performance metrics were calculated on a 10% spatially random testing sample of the data that was not included in model fitting (one of the options for the proportion of testing data for cross-validation on the BIOMOD platform, Thuiller et al. 2009). Two of the sites – Mt Tam

Table 1. Variables included and their native resolutions.

Variable	Acronym	Data source	Native resolution
Interpolated height above a stream	IHAS	Airborne LiDAR	10 m
Curvature		Airborne LiDAR	10 m
Topographic wetness index	TWI	Airborne LiDAR	10 m
Heat load index	HLI	Airborne LiDAR	10 m
Fog frequency		MODIS Satellite	1 km
Soil water storage		USDA Natural Resource Conservation Survey	1457 m^2–37 km^2

and Jackson Forest – had a much higher representation of redwood absences than presences. To report performance measures that evenly assessed the ability of the model to accurately detect both presences and absences, we down-sampled the majority class by selecting a random sample of plots from the redwood absence plots that was the same size as the number of redwood plots prior to model fitting (Evans et al. 2010). For a single site (Mt Tam), models were developed at a range of grain sizes from 10 m × 10 m to 250 m × 250 m, to test for variation in model performance with grain size.

We evaluated two aspects of model performance: discrimination, or the ability to differentiate between presences and absences, and calibration, or the ability to predict the probability of occurrence (Araújo et al. 2019). Discrimination was evaluated with overall accuracy and AUC statistics (Thuiller et al. 2009, Jiménez-Valverde 2012). The maximum overall accuracy from 100 different thresholds between the minimum and the maximum probability was determined. Calibration was assessed with a calibration plot (Pearce and Ferrier 2000). Within each decile of predicted habitat suitability, the proportion of plots with presences was plotted against the decile mean (Fieberg et al. 2018). Points were compared with a line of unity, representing perfect agreement between model predictions of probability of occurrence and the proportion of occurrence (Pearce and Ferrier 2000).

Assessing the influence of different moisture sources

We evaluated the relative importance and the functional relationship of each metric of belowground moisture and fog on redwood distributions. First, we computed the relative influence of each predictor in each BRT model. The relative influence is scaled so that the sum of all relative influences in a single model is equal to 1, and can be interpreted as a ranking of the importance of each variable to the predictions from each model (Elith et al. 2008). We interpreted these variable rankings within the context of the overall performance of each model, the distribution of each variable at each site, and the functional form of the relationship of redwood distributions to each predictor variable at each site. To display the functional forms and distributions, we plotted the mean and bootstrapped 95% percent confidence intervals of redwood density within each decile of each predictor variable. We calculated the confidence interval by drawing 100 random samples of plots within each decile without replacement and calculated the average of each random sample.

Results

Hydrologic niche model performance: discrimination and calibration

Models including spatial variation in access to fog and belowground moisture predicted redwood presence and absence and habitat suitability reasonably well across three landscapes. Spatial variation in access to fog and belowground moisture discriminated between presence and absence of redwoods at the microscale with 65%, 74% and 63% overall accuracy at Big Basin, Mt Tam and Jackson Forest, respectively, and AUC of 0.70 at Big Basin, 0.84 at Mt Tam, 0.68 at Jackson Forest (Table 2). At Mt Tam, model discrimination varied little among models developed at grain sizes of 10 m × 10 m–100 m × 100 m, but showed a modest decline with grain size at grain sizes 150 m × 150 m and coarser (Supplementary material Appendix 2 Fig. A12–A14).

The models correctly predicted the overall trend in the proportion of occurrence (Fig. 2), but in all sites, predicted a smaller range in habitat suitability than the observed proportion of occurrence (compare x-axis range of red points in Fig. 2 with their range on the y-axis). Specifically, the models overpredicted the proportion of occurrence in regions predicted to have low habitat suitability (less than the 4th decile at Big Basin and the 5th decile at Mt Tam and Jackson Forest), and underpredicted the proportion of occurrence in regions predicted to have high habitat suitability (Fig. 2). The models predicted that 10 m plots varied between 22–75% suitability as redwood habitat at Mt Tam, 32–65% at Jackson Forest and 24–70% at Big Basin.

Access to belowground moisture

IHAS was consistently associated with redwood distributions (Fig. 3 and 4). At all three sites, redwood density declined linearly with increasing IHAS (Fig. 4). Redwood density

Table 2. Discrimination performance of a machine learning model predicting the presence and absence of redwoods from five metrics of belowground moisture and fog moisture at three sites. The overall accuracy and AUC calculated on a testing dataset are shown for each of the three sites.

	Overall accuracy	AUC	Sensitivity	Specificity
Big Basin	0.65	0.70	0.80	0.50
Mt Tam	0.74	0.84	0.78	0.73
Jackson Forest	0.63	0.68	0.71	0.55

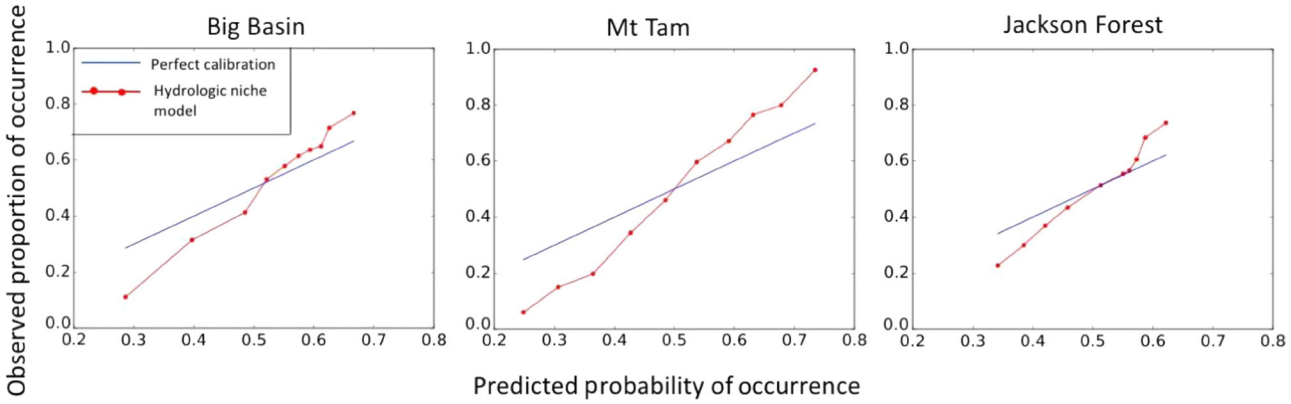


Figure 2. Calibration performance of a classification model predicting the probability of a redwood at three sites from five measures of belowground moisture and fog moisture. The x-axis shows the mean of each decile of predicted probability from the model, and the y-axis shows the proportion within each decile of predicted probability with redwood presence. The red points are the true proportion of occurrence within each decile of predicted probability of occurrence, and the blue line shows perfect agreement between the predicted probability of occurrence and the observed proportion of occurrence.

declined most steeply with increasing IHAS at Big Basin, followed by Jackson Forest and then Mt Tam. Similarly, IHAS was the second most important variable at Big Basin and Jackson Forest and the fourth most important variable at Mt Tam (Fig. 3). Within an 800 m × 800 m area, the interquartile range of 10 m × 10 m IHAS pixels ranged from 25 m to 109 m at Big Basin, 25 m to 94 m at Mt Tam and 5 m to 146 m at Jackson Forest (Supplementary material Appendix 2 Fig. A15–A17). Redwood density increased modestly with increasing TWI and declined with increasing curvature (Fig. 4), and both curvature and TWI were within the three least important variables at all sites (Fig. 3). The effect of HLI on redwood density was variable across the sites (Fig. 4). Soil water storage was the most important variable in redwood distributions at Big Basin. Redwood density increased in response to increasing soil water storage at Big Basin, but its response was variable at the other two sites (Fig. 4).

Access to moisture from fog

The response of redwood density to fog frequency was similar across Mt Tam and Jackson Forest despite differences in the range of fog frequency. Mt Tam showed the highest fog frequency and the largest variability in fog frequency (Fig. 4). At both Mt Tam and Jackson Forest, fog frequency had the highest relative influence in the BRT model, and redwood density generally increased until approximately 15% fog frequency, and then showed a plateau until approximately

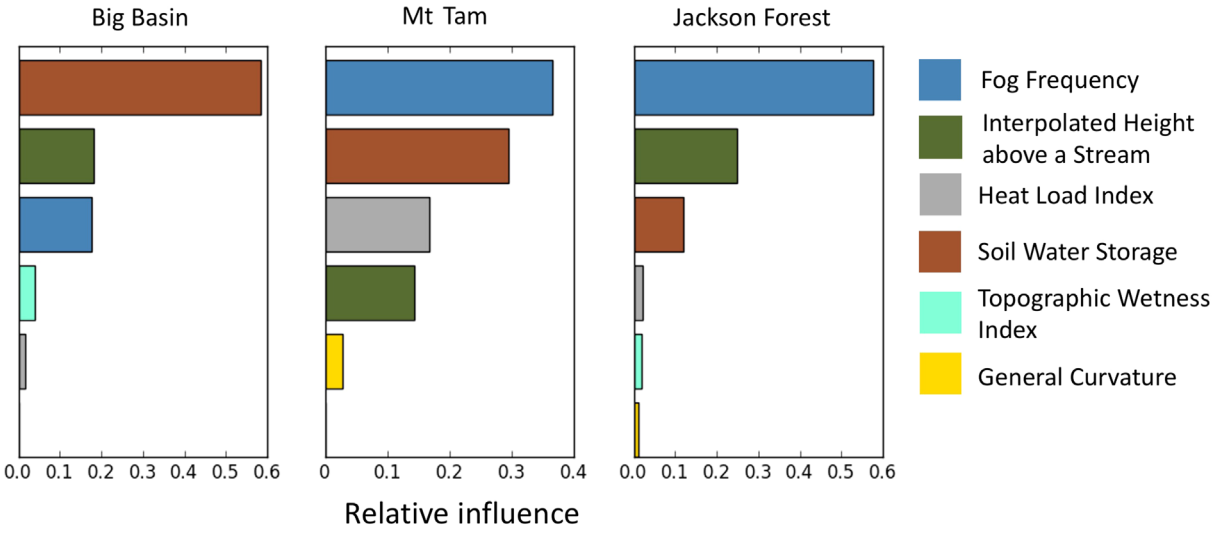


Figure 3. The relative influence of each measure of belowground moisture and fog moisture on redwood probability in a boosted regression tree model at each sites. Barcharts show the relative influence of each predictor variable in modeling probability of occurrence of redwoods. Within each model, the relative influence is the mean improvement that results from each split by each variable, scaled to sum to 1. Relative influences were interpreted within the context of the overall performance of the model predictions for each site shown in Table 2 and Fig. 2, and the responses of redwood distributions to each variable shown in Fig. 4.

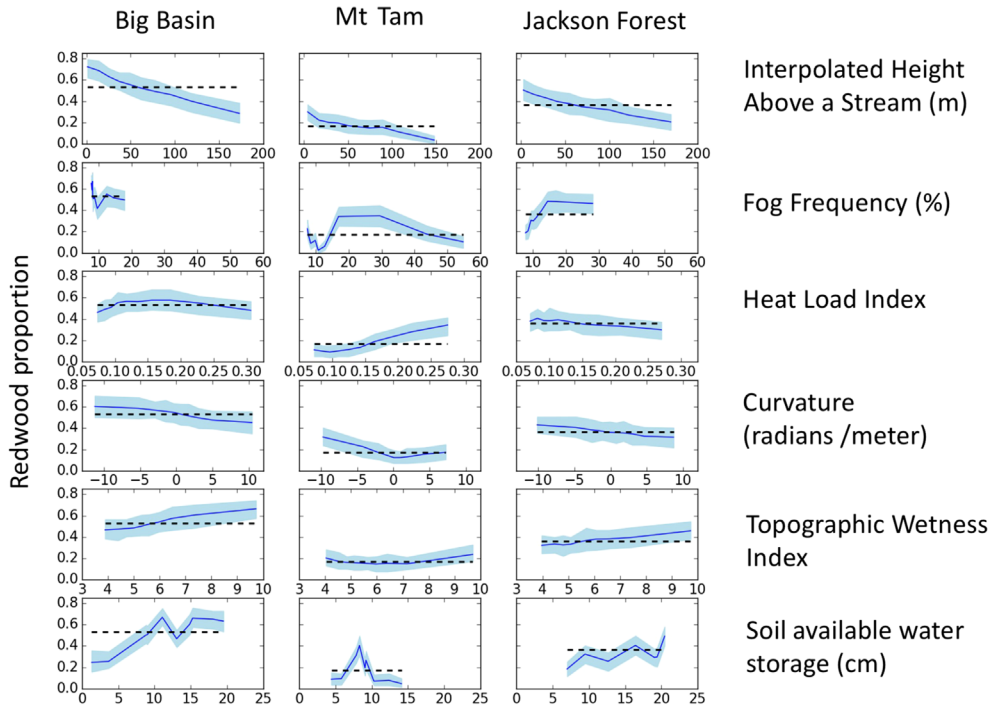


Figure 4. The density of redwoods within each decile of each metric of belowground moisture and fog moisture across the three sites. The dark blue lines show the mean, and blue shaded regions show the bootstrapped 95% percent confidence intervals of redwood density calculated within each decile of each predictor variable. The sitewide mean proportion is shown as a dashed black line for reference. The title of the x-axis for each row of plots is shown on the right side of the plots. Responses across the sites are most similar for the interpolated height above a stream (IHAS, first row of plots), for which redwood density declines consistently with increasing IHAS at all three sites.

30% fog frequency (Fig. 3). At fog frequency above 29% at Mt Tam, redwood density declined (Fig. 4). At Big Basin, fog frequency was the third most important variable to redwood distributions (Fig. 3), and Big Basin had the lowest fog frequency of all the sites. Fog frequency generally declined with increasing distance from the coast at all three sites (Supplementary material Appendix 2 Fig. A8–A10).

Discussion

Topographic gradients in moisture availability, soil water storage and fog frequency predicted significant variability in redwood habitat suitability at the landscape scale. Across all three landscapes, redwood density was consistently elevated in sites close to streams, but the influence of other predictors varied among the sites. The high variability in height above a stream within an 800 m × 800 m area, coupled with the consistent and steep relationship of height above a stream and redwood habitat suitability, suggests that sub-regional scale heterogeneity in access to moisture should be accounted for in predictions of future redwood habitat suitability under climate change.

Landscape-scale variation in water availability predicts redwood habitats

Models including six measures of water availability indicated that spatial variation in access to moisture could predict overall trends in redwood habitat suitability at fine spatial scales. However, the models predicted a smaller range of variation in the proportion of occurrence than was actually observed, (Fig. 2). This type of calibration error is referred to as incorrect spread, and it could be a result of variation due to factors we did not include, or interactions or effects that were not accounted for in the model (Pearce and Ferrier 2000). Error in the redwood presence and absence map could also be contributing (up to 19%, 10%, 2% of redwoods were falsely identified as other species at Jackson Forest, Mt Tam and Big Basin, and up to 3%, 1% and 2% of other species at Jackson Forest, Mt Tam and Big Basin were classified as redwoods, Francis and Asner 2019). We also expect that some of the predictive success of the models could be explained by covariation of the variables we included with other spatially varying factors that we did not include, as discussed below.

Access to belowground moisture influences redwood habitat suitability

The vertical distance of a site above the interpolated stream elevation, measured by IHAS, was consistently negatively associated with redwood density across all three sites (Fig. 4). The steep decline of redwood abundance with increasing IHAS at Big Basin and Jackson Forest was consistent with the ranking of IHAS as the second most influential variable at those sites (Fig. 2). IHAS was a stronger and more consistent

predictor of redwood density than curvature or TWI, indicating its utility as a topographic metric. Low IHAS positions are likely associated with high belowground moisture content through multiple mechanisms, including higher water inputs, increasing proximity to the water table (Fan et al. 2017), increasing soil depth due to physical soil erosion along hillslopes, and increasing soil water storage capacity due to chemical soil erosion along hillslopes (Jenny 1941). Isotopic mixing models from a single forest in Northern California showed that 55–87% of the water used by redwoods during the summer originates from winter precipitation (Dawson 1998), which may be stored belowground as soil, water table and rock moisture (Rempe and Dietrich 2018).

We expected redwood density to be positively related to soil water storage capacity. At Big Basin, soil water storage was the most influential variable in the BRT model (Fig. 3), consistent with the steep increase in redwood density with increasing soil water storage at that site (Fig. 4). The importance of soil water storage at Big Basin was unsurprising given the presence of unique soil deposits with very low water storage at this site (Supplementary material Appendix 1 Supplementary text). The inconsistent response of redwood density to soil water storage at Mt Tam suggests its relatively high influence in the model may stem from a correlation with another variable (Supplementary material Appendix 2 Fig. A2 and A5 and Supplementary material Appendix 1 Supplementary text). We note important limitations of the SSURGO dataset, including potential assumptions about soil types from overlying vegetation made by surveyors, and differences in sampling protocols across survey boundaries (Davis et al. 2010). Recent studies have found that incorporating variation in soil type improves the performance of species distribution models (Coudon et al. 2006, Walthert and Meier 2017, Baudraz et al. 2018). In our case, the lack of consistency of the relationship of soil water storage to redwood habitat suitability across the sites, coupled with the limitations of the SSURGO soil dataset, suggests caution on the use of SSURGO soil water storage data to infer variation in redwood habitat.

The role of spatial variation in fog frequency on redwood habitats

Fog is a source of water for redwoods during summers and drought years (Dawson 1998, Limm et al. 2009, Templer et al. 2015), and the redwood range, at 1 km resolution, is confined to fog-influenced regions (Johnstone and Dawson 2010). We therefore expected that fog frequency would be an important determinant of redwood distributions and that redwood density would be linearly and positively correlated with fog frequency. In keeping with our expectations, fog frequency was ranked as the most important variable in the model at Jackson Forest and at Mt Tam (Fig. 3), and redwood density generally increased from low (approximately 5%) to moderate (approximately 30%) fog frequency at both sites. In contrast with our expectations, high fog frequency (above 30%) corresponded to low redwood densities at Mt Tam (Fig. 4). This may be due to the fact that the sites with the highest fog frequency are also close to the coast (Supplementary material Appendix 2 Fig. A8–A10), and may also be exposed to strong coastal winds and high sea salt deposition (Clayton 1972, Wu and Guo 2006). The low importance of fog frequency in predicting redwood habitats at Big Basin (Fig. 3 and 4) may have been due to the lower fog frequency and smaller range in fog frequency at that site (Supplementary material Appendix 2 Fig. A1 and Supplementary material Appendix 1 Supplementary text). Furthermore, some of the nonlinearity in the relationship of redwood habitat suitability to fog frequency may be due to differences in the type of fog moisture that trees have access to, which our fog frequency map was not able to quantify. For example, trees that are located at elevations that are equal to the height of the fog base are exposed to water inputs from fog drip (Sawaske and Freyberg 2015), whereas those that are located at lower elevations may be exposed only to shading and increased relative humidity (Fischer et al. 2009).

Implications for future habitat suitability of tree species with high conservation value under climate change

A previous SDM study for redwoods using 800 m resolution data predicted that under a middle-of-the-road climate scenario for California, there would be no suitable habitat for redwoods south of the San Francisco Bay by the year 2030 (Fernandez et al. 2015). This includes the entirety of Big Basin, one of the sites included in our study. We found that at the landscape scale, redwood habitat suitability was elevated at sites close to streams (low IHAS), and that the variation in IHAS within an 800 m × 800 m area was substantial (Supplementary material Appendix 2 Fig. A15–A17). Therefore, while we did not predict future redwood distributions under climate change, our findings challenge the assumption that redwood habitat suitability in an 800 m × 800 m area can be described by single value. Reducing uncertainty on whether there are microrefugia within regions that have been predicted to become climatically unsuitable will require quantitative predictions of redwood distributions at fine spatial scales to map suitable and unsuitable habitat under climate change.

Furthermore, our finding that redwood habitat suitability was linked to spatial variability in fog frequency at two of the sites suggests that the possibility of a change in fog frequency under climate change could have a substantial influence on future redwood habitat suitability, despite deep uncertainty on how fog will respond to climate change. While airport records suggest that fog frequency has declined by 33% over the past century (Johnstone and Dawson 2010), there is modest evidence of a strengthened coastal-to-inland temperature gradient (Cordero et al. 2011), which would be expected to correspond to an increase in fog frequency. Predictions of the impact of climate change on fog frequency that incorporate the role of sea surface temperatures on fog formation (Johnstone and Dawson 2010), and the role of

land temperature in the advection of fog inland and fog base height are needed to reduce uncertainty.

Advantages, limitations and potential of tree species distribution modeling from airborne remote sensing

Our redwood habitat suitability analysis used a tree species presence and absence map derived from airborne imaging spectroscopy. In contrast to SDM studies that have used field-collected species occurrence data (Jetz et al. 2012), this approach enabled us to measure redwood presence and absence at a fine spatial scale over a larger area than would have been practical to sample continuously in field surveys. In addition, this approach significantly reduced the uncertainty about whether the absence of occurrence was due to true absence or lack of sampling (Phillips et al. 2009). As a limitation to the widespread application of this approach, only high-accuracy maps should be used in habitat suitability models to minimize the effects of error propagation. Producing accurate maps may not be possible for many species that are spectrally similar to neighboring species, and even for spectrally distinguishable species, requires large amounts of training data and high-quality imaging spectroscopy data. In cases where the accuracy is sufficient, maps of tree species distributions derived from airborne imaging spectroscopy could uncover consequential variation in habitat suitability at a resolution and extent that is not well-represented in regional-scale tree species distribution models (McKenney et al. 2007).

Conclusion

Topographic gradients in belowground moisture, soil water storage and fog frequency predicted significant variation in redwood habitat suitability at the landscape scale. Across three distinct landscapes spanning a latitudinal gradient, redwood density was elevated at low IHAS positions (close to streams), but the influence of other topographic and edaphic factors varied among the three landscapes. We found substantial variation in IHAS within an area equal to the grain sizes used in previous species distribution models for redwoods, indicating that landscape scale gradients in access to moisture may moderate future spatial patterns of redwood habitat suitability under climate change. Future research should predict redwood habitat suitability at fine spatial scales to identify potential microrefugia within regions that have been predicted to become climatically-unsuitable for redwoods at a regional scale. Airborne remote sensing could contribute to understanding of tree species' responses to climate change, by providing high-resolution maps of tree species distributions and topography at the landscape scale.

Data availability statement

Data available from the Dryad Digital Repository: <https://doi.org/10.5061/dryad.fbg79cns5> (Francis et al. 2020).

Acknowledgements – We thank the staff of the Global Airborne Observatory for assistance in data collection and processing and Phil Brodrick for help with IHAS mapping. This manuscript was improved through conversations with Phil Brodrick, edits suggested by Reuben Veek, and engaged feedback from two reviewers.
Funding – Airborne remote sensing data collection and processing were funded by the David and Lucile Packard Foundation and the John D. and Catherine T. MacArthur Foundation. The Global Airborne Observatory is made possible by support by private foundations, visionary individuals, and Arizona State Univ. EJF was funded by a Stanford Graduate Fellowship in Science and Engineering. Field work to develop the redwood presence absence map was funded by the Save the Redwoods League Grant #10674.
Author contributions – EJF, GPA, KJM and CBF designed the study, GPA collected the airborne imaging spectroscopy and LiDAR data, EJF performed the analyses, EJF, KJM and CBF interpreted the results, EJF drafted the manuscript, EJF, KJM, CBF and GPA edited the manuscript.
Conflicts of interest – The authors declare that they have no conflict of interest.

References

Allen, C. D. et al. 2010. A global overview of drought and heat-induced tree mortality reveals emerging climate change risks for forests. – For. Ecol. Manage. 259: 660–684.

Anderegg, W. R. L. et al. 2013. Consequences of widespread tree mortality triggered by drought and temperature stress. – Nat. Clim. Change. 3: 30–36.

Anderegg, W. R. L. et al. 2019. Widespread drought-induced tree mortality at dry range edges indicates that climate stress exceeds species' compensating mechanisms. – Global Change Biol. 25: 3793–3802.

Andrew, M. E. and Ustin, S. L. 2009. Habitat suitability modeling of an invasive plant with advanced remote sensing data. – Divers. Distrib. 15: 627–640.

Araújo, M. B. et al. 2019. Standards for distribution models in biodiversity assessments. – Sci. Adv. 5: 1–11.

Asner, G. P. et al. 2012. Carnegie Airborne Observatory-2: increasing science data dimensionality via high-fidelity multi-sensor fusion. – Remote Sens. Environ. 124: 454–465.

Baguskas, S. A. et al. 2014. Evaluating spatial patterns of drought-induced tree mortality in a coastal California pine forest. – For. Ecol. Manage. 315: 43–53.

Baldeck, C. A. et al. 2015. Operational tree species mapping in a diverse tropical forest with airborne imaging spectroscopy. – PLoS One 10: e0118403.

Baudraz, M. E. A. et al. 2018. Learning from model errors: can land use, edaphic and very high-resolution topo-climatic factors improve macroecological models of mountain grasslands? – J. Biogeogr. 45: 429–437.

Beven, K. J. and Kirkby, M. J. 1979. A physically based, variable contributing area model of basin hydrology/Un modèle à base physique de zone d'appel variable de l'hydrologie du bassin versant. – Hydrol. Sci. Bull. 24: 43–69.

Breshears, D. D. et al. 2013. The critical amplifying role of increasing atmospheric moisture demand on tree mortality and associated regional die-off. – Front. Plant. Sci. 4: 266.

Carroll, A. L. S. et al. 2014. Millenium-scale crossdating and interannual climate sensitivities of standing California redwoods. – PLoS One 9: e102545.
Clayton, J. L. 1972. Salt spray and mineral cycling in two California coastal ecosystems. – Ecology 53: 74–81.
Cordero, E. C. et al. 2011. The identification of distinct patterns in California temperature trends. – Clim. Change 108: 357–382.
Coudon, C. et al. 2006. Soil nutritional factors improve models of plant species distribution: an illustration with *Acer campestre* in France. – J. Biogeogr. 33: 1740–1763.
Cushman, S. A. et al. 2010. The gradient paradigm: a conceptual and analytical framework for landscape ecology. – In: Cushman, S. A. and Huettman, F. (eds), Spatial complexity, informatics and wildlife conservation. Springer, pp. 83–108.
Daly, C. et al. 2008. Physiographically-sensitive mapping of temperature and precipitation across the coterminous United States. – J. Appl. Meterol. Climatol. 33: 140–158.
Davis, F. W. et al. 2010. Pre-impact forest composition and ongoing tree mortality associated with sudden oak death in the Big Sur region; California. – For. Ecol. Manage. 259: 2342–2354.
Dawson, T. E. 1990. Spatial and physiological overlap of three co-ocurring alpine willows. – Funct. Ecol. 4: 13–25.
Dawson, T. E. 1998. Fog in the California redwood forest: ecosystem inputs and use by plants. – Oecologia 117: 476–485.
Dobrowski, S. Z. 2011. A climatic basis for microrefugia: the influence of terrain on climate. – Global Change Biol. 17: 1022–1035.
Douda, J. et al. 2012. Plant species coexistence at local scale in temperate swamp forest: test of habitat heterogeneity hypothesis. – Oecologia 169: 523–534.
Elith, J. and Graham, C. H. 2009. Do they? How do they? Why do they differ? On finding reasons for differing performances of species distribution models. – Ecography 32: 66–77.
Elith, J. and Leathwick, J. R. 2009. Species distribution models: ecological explanation and prediction across space and time. – Annu. Rev. Ecol. Evol. Syst. 40: 677–697.
Elith, J. et al. 2008. A working guide to boosted regression trees. – J. Anim. Ecol. 77: 802–813.
Evans, J. S. et al. 2010. Modeling species distribution and change using Random Forest. – In: Drew, C. A. et al. (eds), Predictive species and habitat modeling in landscape ecology. Springer, pp. 139–159.
Fan, Y. et al. 2017. Hydrologic regulation of plant rooting depth. – Proc. Natl Acad. Sci. USA 114: 10572–10577.
Fernandez, M. et al. 2015. Back to the future: using historical climate variation to project near-term shifts in habitat suitable for coast redwood. – Global Change Biol. 21: 4141–4152.
Fieberg, J. R. et al. 2018. Used-habitat calibration plots: a new procedure for validating species distribution, resource selection and step-selection models. – Ecography 41: 737–752.
Fischer, D. T. et al. 2009. Significance of summer fog and overcast for drought stress and ecological functioning of coastal California endemic plant species. – J. Biogeogr. 36: 783–799.
Francis, E. J. and Asner, G. P. 2019. High-resolution mapping of redwood (*Sequoia sempervirens*) distributions in three Californian forests. – Remote Sens. 11: 1–19.
Francis, E. J. et al. 2020. Data from: Landscape scale variation in the hydrologic niche of California coast redwood. – Dryad Digital Repository, <https://doi.org/10.5061/dryad.fbg79cns5>.
Franklin, J. et al. 2013. Modeling plant species distributions under future climates: how fine scale do climate projections need to be? – Global Change Biol. 19: 473–483.
García-Baquero, G. et al. 2016. Dissecting the hydrological niche: soil moisture, space and lifespan. – J. Veg. Sci. 27: 219–226.
Grinnell, J. 1917. The niche-relationships of the California thrasher. – AOS 49: 427–433.
Guisan, A. and Thuiller, W. 2005. Predicting species distribution: offering more than simple habitat models. – Ecol. Lett. 8: 993–1009.
He, K. S. et al. 2015. Will remote sensing shape the next generation of species distribution models? – Remote Sens. Ecol. Conserv. 1: 4–18.
Heikkinen, R. K. et al. 2012. Does the interpolation accuracy of species distribution models come at the expense of transferability? – Ecography 35: 276–288.
Iacobellis, S. F. and Cayan, D. R. 2013. The variability of California summertime marine stratus: impacts on surface air temperatures. – J. Geophys. Res. Atmos. 118: 9105–9122.
IPCC 2013. Climate change 2013: the physical science basis. Contribution of Working Group I to the Fifth Assessment Report of the Intergovernmental Panel on Climate Change. – Cambridge Univ. Press.
Iverson, L. et al. 2013. Estimating potential habitat for 134 eastern US tree species under six climate scenarios. – For. Ecol. Manage. 254: 390–406.
Jenny, H. 1941. Factors of soil formation, a system of quantitative pedology. – McGraw-Hill.
Jetz, W. et al. 2012. Integrating biodiversity distribution knowledge: toward a global map of life. – Trends Ecol. Evol. 27: 151–159.
Jiménez-Valverde, A. 2012. Insights into the area under the receiver operating characteristic curve (AUC) as a discrimination measure in species distribution modelling. – Global Ecol. Biogeogr. 21: 498–507.
Johnstone, J. A. and Dawson, T. E. 2010. Climatic context and ecological implications of summer fog decline in the coast redwood region. – Proc. Natl Acad. Sci. USA 107: 4533–4538.
Koch, G. W. et al. 2004. The limits to tree height. – Nature 428: 851–854.
Lenoir, J. et al. 2017. Climatic microrefugia under anthropogenic climate change: implications for species redistribution. – Ecography 40: 253–266.
Letten, A. D. et al. 2015. Fine-scale hydrological niche differentiation through the lens of multi-species co-occurrence models. – J. Ecol. 103: 1264–1275.
Limm, E. B. et al. 2009. Foliar water uptake: a common water acquisition strategy for plants of the redwood forest. – Oecologia 161: 449–459.
Little, E. 1971. Atlas of United States trees. – US Dept of Agriculture Forest Service.
Loarie, S. R. et al. 2009. The velocity of climate change. – Nature 462: 1052–1055.
McCune, B. and Dylan, K. 2002. Equations for potential annual direct incident radiation and heat load. – J. Veg. Sci. 13: 603–606.
McKenney, D. W. et al. 2007. Potential impacts of climate change on the distribution of North American trees. – BioScience 57: 939–948.
McLaughlin, B. C. et al. 2017. Hydrologic refugia, plants and climate change. – Global Change Biol. 23: 2941–2961.

Meier, E. S. et al. 2011. Climate, competition and connectivity affect future migration and ranges of European trees. – Global Ecol. Biogeogr. 21: 164–178.
Moore, I. D. et al. 1991. Digital terrain modelling: a review of hydrological, geomorphological and biological applications. – Hydrol. Process 5: 3–30.
Morin, X. and Thuiller, W. 2009. Comparing niche- and process-based models to reduce prediction uncertainty in species range shifts under climate change. – Ecology 90: 1301–1313.
Nobre, A. D. et al. 2011. Height above the nearest drainage – a hydrologically relevant new terrain model. – J. Hydrol. 404: 13–29.
O'Callaghan, J. F. and Mark, D. M. 1984. The extraction of drainage networks from digital elevation data. – Comp. Vis. Graph. Imag. Process 28: 323–344.
Pearce, J. and Ferrier, S. 2000. Evaluating the predictive performance of habitat models developed using logistic regression. – Ecol. Model. 133: 225–245.
Pedregosa, F. et al. 2011. Scikit-learn: machine learning in Python. – J. Mach. Learn Res. 12: 2825–2830.
Phillips, S. J. et al. 2009. Sample selection bias and presence-only distribution models: implications for background and pseudo-absence data. – Ecol. Appl. 19: 181–197.
Porres de la Haza, M. J. and Pardo Pascual, J. E. 2002. Comparison between the different curvature models of terrain for determining the degree of soil humidity. – In: Sobrino, J. A. (ed.), Recent advances in quantitative remote sensing. Publicaciones de la Univ. de Valéncia, pp. 238–245.
Pradervand, J.-N. et al. 2014. Very high resolution environmental predictors in species distribution models: moving beyond topography? – Prog. Phys. Geogr. 38: 79–96.
Rempe, D. M. and Dietrich, W. E. 2018. Direct observations of rock moisture, a hidden component of the hydrologic cycle. – Proc. Natl Acad. Sci. USA 115: 2664–2669.
Sawaske, S. R. and Freyberg, D. L. 2015. Fog, fog drip and streamflow in the Santa Cruz Mountains of the California Coast Range. – Ecohydrology 8: 695–713.
Silvertown, J. et al. 1999. Hydrologically defined niches reveal a basis for species richness in plant communities. – Nature 400: 61–62.
Silvertown, J. et al. 2015. Hydrological niches in terrestrial plant communities: a review. – J. Ecol. 103: 93–108.
Soberon, J. 2007. Grinnellian and Eltonian niches and geographic distributions of species. – Ecol. Lett. 10: 1115–1123.
Soil Survey Staff 2004. Soil Survey Geographic Database (SSURGO). – <https://websoilsurvey.nrcs.usda.gov>.
Templer, P. H. et al. 2015. Fog as a source of nitrogen for redwood trees: evidence from fluxes and stable isotopes. – J. Ecol. 103: 1397–1407.
Thuiller, W. et al. 2005. Climate change threats to plant diversity in Europe. – Proc. Natl Acad. Sci. USA 12: 8245–8250.
Thuiller, W. et al. 2009. BIOMOD – a platform for ensemble forecasting of species distributions. – Ecography 32: 369–373.
Vaughn, N. R. et al. 2015. Multiple scales of control on the structure and spatial distribution of woody vegetation in African savanna watersheds. – PLoS One 10: e0145192.
Walthert, L. and Meier, E. S. 2017. Tree species distribution in temperate forests is more influenced by soil than by climate. – Ecol. Evol. 7: 9473–9484.
Wu, L. and Guo, X. 2006. Response of two coast redwood (*Sequoia sempervirens* Endl.) varieties to moderate levels of salt and boron spray measured by stress symptoms: implications for landscape irrigation using recycled water. – Environ. Expl. Bot. 58: 130–139.
Zhu, K. et al. 2012. Failure to migrate: lack of tree range expansion in response to climate change. – Global Change Biol. 18: 1042–1052.

Supplementary material (Appendix ECOG-5080 at <www.ecography.org/appendix/ecog-05080>). Appendix 1–2.